

Evaluation of dosimetric advantages of using patient-specific aperture system with intensity-modulated proton therapy for the shallow depth tumor

Keisuke Yasui^{1,2} | Toshiyuki Toshito¹ | Chihiro Omachi¹ | Kensuke Hayashi¹ |
Kenichiro Tanaka¹ | Kumiko Asai¹ | Akira Shimomura¹ | Rie Muramatsu¹ |
Naoki Hayashi²

¹Nagoya Proton Therapy Center, Nagoya City West Medical Center, Nagoya, Japan

²School of Health Sciences, Faculty of Radiological Technology, Fujita Health University, Toyoake, Japan

Author to whom correspondence should be addressed. Keisuke Yasui
E-mail: k-yasui@fujita-hu.ac.jp

Abstract

In this study, we evaluate dosimetric advantages of using patient-specific aperture system with intensity-modulated proton therapy (IMPT) for head and neck tumors at the shallow depth. We used four types of patient-specific aperture system (PSAS) to irradiate shallow regions less than 4 g/cm² with a sharp lateral penumbra. Ten head and neck IMPT plans with or without aperture were optimized separately with the same 95% prescription dose and same dose constraint for organs at risk (OARs). The plans were compared using dose volume histograms (DVHs), dose distributions, and some dose indexes such as volume receiving 50% of the prescribed dose (V_{50}), mean or maximum dose (D_{mean} and D_{max}) to the OARs. All examples verified in this study had decreased V_{50} and OAR doses. Average, maximum, and minimum relative reductions of V_{50} were 15.4%, 38.9%, and 1.0%, respectively. D_{max} and D_{mean} of OARs were decreased by 0.3% to 25.7% and by 1.0% to 46.3%, respectively. The plans with the aperture over more than half of the field showed decreased V_{50} or OAR dose by more than 10%. The dosimetric advantage of patient-specific apertures with IMPT was clarified in many cases. The PSAS has some dosimetric advantages for clinical use, and in some cases, it enables to fulfill dose constraints.

PACS

87.56.nk

KEY WORDS

aperture, IMPT, lateral penumbra, proton beam, spot scanning.

1 | INTRODUCTION

In recent years, accelerators, irradiation control systems, and treatment planning systems have been improved and, as a result of these improvements, scanning proton therapy systems have become more widely used.¹ In spot scanning irradiation, a monoenergetic beam is delivered

to a given spot at the target volume specified in the treatment plan and a full scan across the target volume and the dose distribution in the depth direction is formed by multiple monoenergetic beams.² The energy generated by a commercially available accelerator for proton therapy has a lower limit of approximately 4 g/cm² water equivalent penetration because of the stability of the accelerator, beam efficiency,

This is an open access article under the terms of the Creative Commons Attribution License, which permits use, distribution and reproduction in any medium, provided the original work is properly cited.

© 2017 The Authors. *Journal of Applied Clinical Medical Physics* published by Wiley Periodicals, Inc. on behalf of American Association of Physicists in Medicine.

and effective spot size. This limitation complicates the treatment planning so correspond to this limitation. One method to irradiate shallower regions less than 4 g/cm^2 is to use an energy absorber (EA); however, the monoenergetic beam with an EA has a large spot size due to scattering and has a limited ability to make sharp lateral penumbra, worsening the dose distribution. Although in some cases the scanning method has some issues with the lateral penumbra, it has some advantages over the passive method and x-ray treatment, and a number of studies using scanning proton beams reported dose comparisons of passive beam and x-ray beam^{3,4} or verification of the relative biological effectiveness (RBE).⁵ Flexibility of scanning technique allows for various irradiation methods, and these methods can improve the dose distribution. Developments in treatment planning systems (TPS), treatment machines, and treatment techniques permit the use of intensity-modulated proton therapy (IMPT) for various tumor sites.^{6,7}

Figure 1 shows the archived spot sizes with or without EA that were retrieved from the Hitachi ProBeat III operating in the Nagoya Proton Therapy Center (NPTC),⁸ and these data were presented in a previous paper.⁹ Without the EA, the maximum spot size in air was 13.8 mm at the isocenter plane and the minimum range was 4 g/cm^2 . Regions below 4 g/cm^2 could be irradiated using EA, but the spot size of minimum range was more than 26.7 mm. These bigger lateral penumbras mean a worse dose distribution.^{10,11} To avoid these issues, a variety of useful methods, such as advanced optimize method (contour scanning),¹² improvement of beam line,¹³ and various type of aperture or collimator,^{14–17} have been proposed. In the same way, methods to reduce spot size owing to close the bolus or nozzle to patient were also reported.^{18,19} These methods enable to achieve a sharp lateral penumbra, better dose distribution, and lower out-of-field dose. Although various useful methods were reported in recent years, we started scanning treatment with a patient-specific aperture system (PSAS) in May 2016 to irradiate shallow regions and to obtain sharp lateral penumbras. The PSAS has some downsides that require patient-specific manufacture and the weight of aperture is a burden to therapists. However, the treatment procedures and QA of the PSAS methods were the same as those with non-PSAS methods. Furthermore, PSAS methods do not require complicate equipment and machine maintenance such as MLC, so it is easy to apply PSAS in a clinical setting. In the previous study, we presented verification results of the PSAS for the spot scanning beam and the results showed that PSAS reduced the lateral penumbra by 30%–70% in the simple case.⁹ The PSAS can be used with both single-field uniform dose (SFUD) and IMPT, but the dosimetric advantage of the patient-specific aperture for IMPT has not been clarified. In this study, we clarified the dosimetric advantage of the aperture for IMPT using DVH, dose distribution, and some dose indexes.

2 | MATERIALS AND METHODS

2.A | Scanning delivery system with PSAS

The spot size of the proton beam increases because of scattering by the materials in the beam nozzle and the distance from the exit of beam transport system to the isocenter. Each spot is controlled by

scanning magnet and the maximum field size is $30 \times 30 \text{ cm}^2$ in the NPTC. Ninety-five energies are available for the scanning treatment that are ranging from 71.6 to 221.4 MeV, resulting in water equivalent penetration depths of $4\text{--}30.6 \text{ g/cm}^2$ at intervals of 0.1 g/cm^2 at low energy beam and 0.6 g/cm^2 at high energy beam. The irradiation system is able to use a range shifter from 0.1 to 0.5 g/cm^2 for fine adjustment of the range of high or middle energy beams. The lateral penumbra is generally affected by the distance from the collimator to the surface, depth, beam energy, and energy absorber thickness. Thus, we designed four types of PSAS with different field sizes and distances from the isocenter to put the aperture closer to the patient's body surface. Small PSASs allowed access over the patient's body or patient's immobilization devices for small tumors. The EA had 4 g/cm^2 water equivalent thickness. The maximum water equivalent penetration with PSAS was restricted to 15 g/cm^2 because the patient-specific aperture was made from 3-cm thick brass. Figure 2 and Table 1 showed schematic view and fundamental parameters of the four types of PSASs. The field sizes of the large PSASs (Types 1 and 2) and small PSASs (Types 3 and 4) were $25 \times 25 \text{ cm}^2$ and $10 \times 10 \text{ cm}^2$, respectively. The distance from the isocenter to the aperture was 150–345 mm. As Types 2 and 4 had the same isocenter-to-aperture distance, the spot sizes were the same and the largest spot size was 18.9 mm. Type 1 shows the largest spot size that is 26.7 mm.

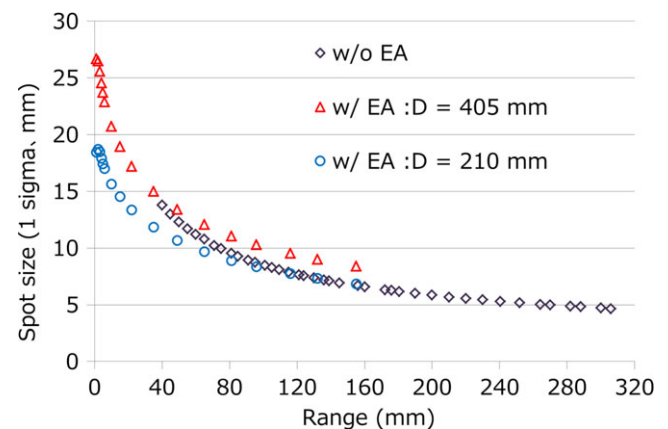


FIG. 1. Air spot sizes (1σ) in the plane of the isocenter versus range. Data are measured with (w/) or without (w/o) the EA. D is the distance from the EA to the isocenter.

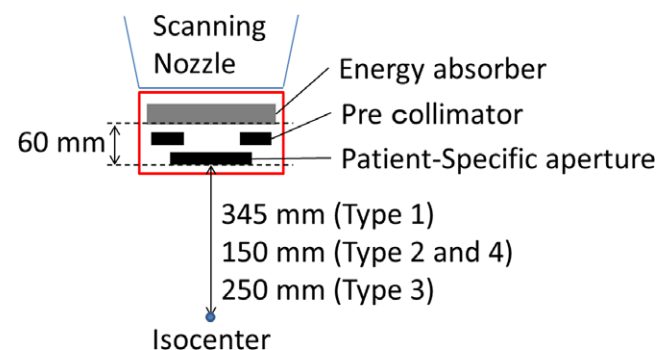


FIG. 2. Schematic view of PSAS.

2.B | Treatment planning and patient selection

TPS used in this study was VQA ver. 3.0.1 (Hitachi Ltd.). The VQA is a commercially available TPS in Japan. The VQA was used for spot scanning with or without PSAS. The VQA system uses a pencil beam algorithm with the triple Gaussian (TG) kernel model to improve the accuracy of dose calculation for the scanning beam.²⁰ In order to handle the aperture, a fluence dose model²¹ was used. The dose calculation with PSAS has sufficiently high-accuracy and details of commissioning results were showed in our previous study.⁹

Ten head and neck (HN) tumor cases treated by IMPT technique with the PSAS in NPTC were examined. HN tumors are a suitable region for this scanning method because most HN tumors have a complex geometry and CTV close to organ at risks (OARs). In this study, the target volumes ranged from 14.33 to 260.02 cm³ and tumor types were nasal cavity, sinus cavity, mandible, base of skull, and oral cavity. Beam angles of each plan were selected considering clinical conditions such as tumor location, tumor size, and OARs. We created IMPT plans with PSASs for actual patient treatment and without apertures for plan comparison. These plans were optimized separately with the same D₉₅ prescription dose and same dose constraint for OAR. The same number of fields and gantry angles were used for each plan and higher priority set to the D₉₅ prescription dose. As mentioned earlier, some fields could not use the PSAS because the PSAS has mechanical limitations such as maximum penetration depth, field size, distance from the isocenter and collision with other devices or the patient. In this study, 12 fields could not use PSAS. These 12 fields consisted of four exceeded penetration depth limit fields and eight fields that have mechanical collision between outer frame of PSAS and patient or treatment couch. The treatment plan information is listed in Table 2. All PSAS fields including without aperture fields listed in Table 2 were using the EA. We used a worst case optimization²² for dose optimization to obtain the robust plan. Parameters of the worst case optimization were 3 mm for x, y, z direction and 3.5% for range uncertainty,²³ so 9 scenarios were considered to the target and OARs. The value of 3 mm is the uncertainty of patient setup for HN tumor and machine variability in NPTC. The value of 3.5% is range uncertainty resulting from uncertainties of the range calculation, the acquisition of CT number, and CT number-Stopping power conversion table. CT images were acquired and reconstructed with 1 mm slices. In the aperture field, the aperture margin was required to assure the marginal dose of the target. The aperture margin was computed by expanding of the maximum outline of the target from the beam's eye view and the margin set to the same value as the spot

spacing. The spot spacing was affected by spot size, so the aperture margin was being from 7.2 mm to 11.2 mm at isocenter.

2.C | Plan evaluation

We compared with- and without aperture plans using dose volume histogram (DVH), dose distribution, and some dose indexes. As mentioned earlier, we made with- or without aperture plans with the same target dose so that the 95% dose to the target was equal. In this study, we used relative reduction of some dose indexes such as volume receiving 50% of the prescribed dose (V₅₀) and maximum dose (D_{max}) or mean dose (D_{mean}) to the OARs. V₅₀ was used for estimate to the out-of-field dose. The relevant OARs of each plan were varied so we evaluated the relevant OARs as described in Table 2. Lens, optic nerve, brain stem, chiasm, and eye were analyzed using D_{max}. Parotid, tongue and brain were analyzed by D_{mean}.

3 | RESULTS

Figure 3 shows examples of DVHs with and without aperture. The results show that the target doses were almost equal and some OARs doses were reduced. The most effective case was plan ID 6, in which V₅₀ was decreased by 35.9%. In contrast, in plan ID 5, an ineffective case, V₅₀ was decreased by only 3.6%. Figure 4 shows examples of dose distribution for both effective and ineffective cases. In the effective case of Fig. 4, all fields can use aperture and apertures are close to the patient surface, as results of which these plans have obviously sharp penumbras. Figure 5 shows the relative difference of V₅₀ and D_{max} or D_{mean} between with and without aperture. All examples verified in this study showed decreased V₅₀ and OAR doses. The average, maximum, and minimum relative reductions of V₅₀ were 15.4%, 38.9%, and 1.0%, respectively. The relative reductions of V₅₀, D_{max}, and D_{mean} are summarized in Fig. 5. D_{max} and D_{mean} of OARs were decreased by 0.3% to 25.7% and by 1.0% to 46.3%, respectively. Plan IDs 2, 3, 6–9 used apertures for more than half of fields and decreased V₅₀ or OAR doses more than 10%. In plan ID 6, D_{max} of the chiasm decreased from 51.3 to 38.2 GyE (25.7%) and D_{mean} of the brain was decreased by 36.2%. The relative reduction of parotid D_{mean} in plan ID 3 was 45.3%. The dose constraints of the OARs of these plans were only fulfilled using aperture plans. At the same time, our PSASs have a maximum penetration depth and mechanical interference limitations so we could not use apertures for all fields. Plan IDs 1, 4, 5, and 10 could only use apertures for not more than half of fields because of the tumor depth or mechanical collision, so these cases showed only small effects.

TABLE 1 Fundamental parameters of the four types of PSAS.

Type	Field size (cm ²)	Distance from the isocenter (mm)		Maximum spot size (mm)
		To aperture	To absorber	
1	25 × 25	345	405	26.7
2	25 × 25	150	210	18.9
3	10 × 10	250	310	22.9
4	10 × 10	150	210	18.9

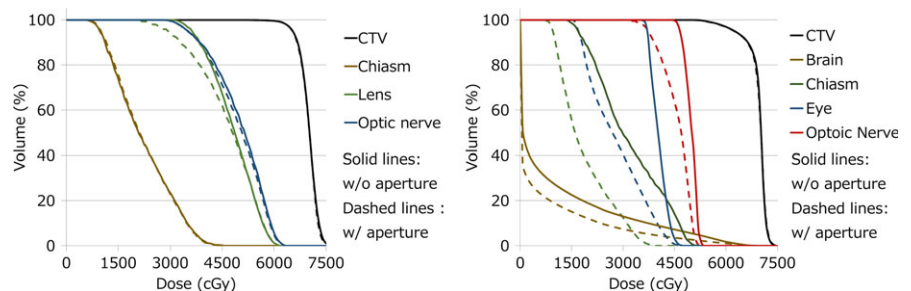
4 | DISCUSSION

This study investigated the dosimetric advantages of the patient-specific aperture to HN IMPT. The patient-specific aperture reduced

TABLE 2 Plan information with fields, gantry angle, prescribed dose, CTV volume, and OAR.

ID	Gantry angle (°)	Aperture type	Field aperture/all	Energy range (MeV)	Prescribed dose (GyE)	CTV volume (cc)	OAR
1	0	Type 2	1/3	142.7–76.2	60.8	258.9	Lens
	120	Non		161.1–71.6			Optic nerve
	240	Non		163.4–71.6			Parotid
2	30	Type 3	3/3	144.4–81.4	70.2	14.3	Parotid
	90	Type 3		135.8–76.2			
	140	Type 4		146.3–77.9			
3	30	Type 4	3/4	135.8–76.2	70.2	145.6	Parotid
	65	Type 3		130.5–76.2			Tongue
	105	Type 1		130.5–77.0			
	195	Non		173.3–107.3			
4	55	Type 3	2/4	137.5–71.6	70.2	58.2	Brain
	305	Type 3		146.3–76.2			Brain stem
	115	Non		163.4–105.9			Chiasm
	260	Non		168.3–104.5			
5	0	Type 3	1/3	148.3–76.2	70.2	260.0	Chiasm
	130	Non		154.8–71.6			Lens
	230	Non		175.7–80.5			Optic nerve
6	0	Type 1	4/4	159–76.2	70.2	150.5	Brain
	300	Type 1		168.3–76.2			Chiasm
	100	Type 4		146.3–76.2			Eye
	260	Type 4		159–76.2			Optic nerve
7	0	Type 4	2/3	146.3–79.7	70.2	45.5	Brain stem
	130	Non		170.8–112.7			Chiasm
	260	Type 1		148.3–96.1			Eye, optic nerve
8	0	Type 4	2/3	154.8–77.9	70.2	60.7	Brain stem
	110	Type 3		165.7–93.5			Chiasm
	240	Non		163.4–81.4			Eye, optic nerve
9	0	Type 2	3/4	144.4–76.2	70.2	137.8	Brain
	40	Type 2		168.3–76.2			Parotid
	180	Non		175.7–107.3			
	320	Type 2		168.3–76.2			
10	0	Type 2	1/3	152.6–76.2	70.2	211.5	Brain stem
	120	Non		168.3–71.6			Chiasm
	240	Non		168.3–71.6			Eye, optic nerve

FIG. 3. Examples of DVHs of an effective case (left) and an ineffective case (right). Left example is plan ID 6 and right example is plan ID 5. Solid lines are without (w/o) aperture and dashed lines are with (w/) aperture.



V_{50} and OAR doses as shown in Figs. 3–5 even when using IMPT. Plan dose constraints of ID 2, 6, 7 only fulfilled with the aperture plan and other plans can reduce unnecessary out-of-field dose. The

decrease rate of D_{max} in some cases was dramatic but other cases showed small effects because OARs were close to the CTV. In this study, we optimized plans while prioritizing the target dose so many

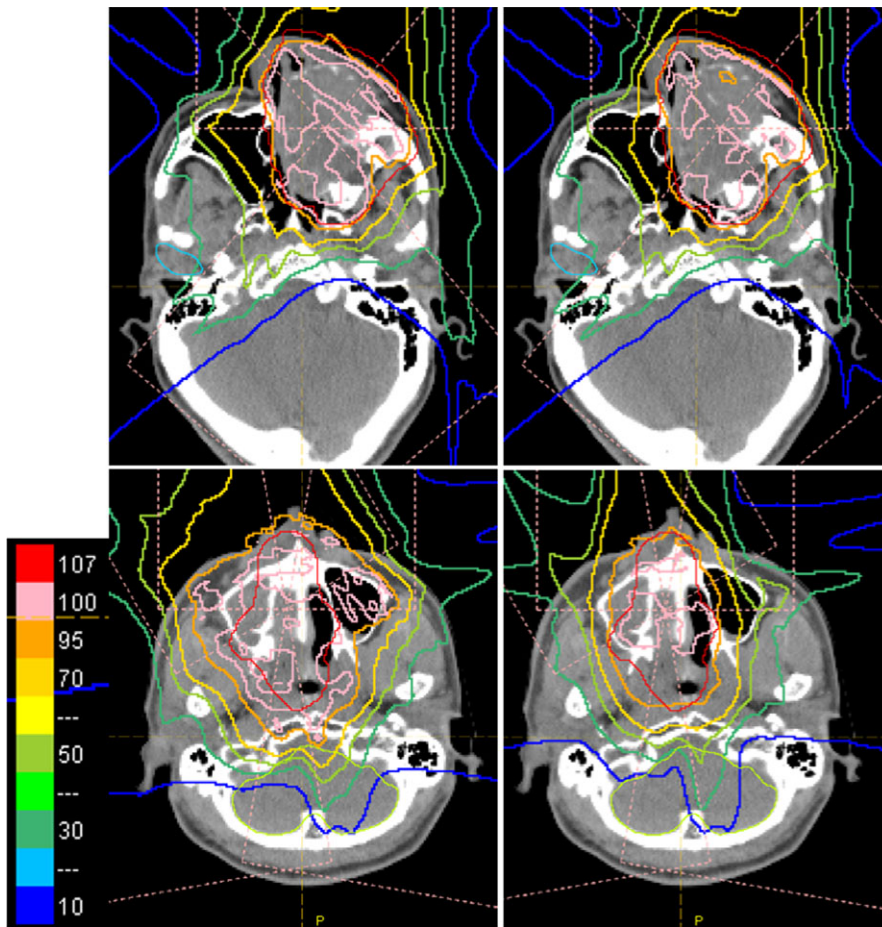


FIG. 4. Examples of dose distribution of the ineffective case (upper) and effective case (lower). Upper example is plan ID 5 and lower example is plan ID 6. Right side of each case is with aperture and left side is without aperture. There are same plans shown in Fig. 3.

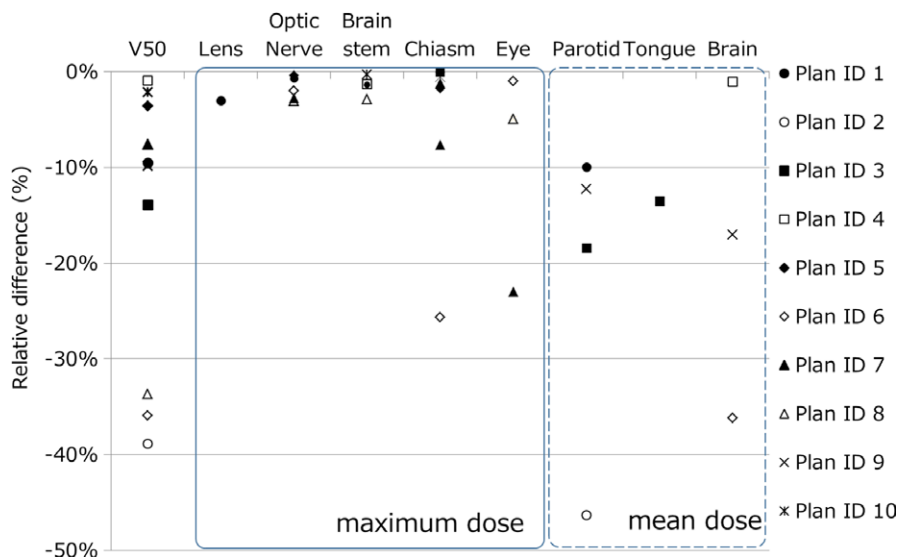


FIG. 5. Relative reductions of V_{50} , D_{max} , and D_{mean} OAR doses between with and without aperture.

maximum dose OARs showed minimal change. In addition, the aperture only collimates the outer line of the target from each beam's eye view and the current optimization algorithm of our TPS cannot consider OAR blocking when using the aperture. In the IMPT plan, the results might be improved by using OAR blocking with an aperture for each field. From the results of our study, using more than half of fields was needed to obtain effective results.

We clarified the dosimetric advantage of patient-specific apertures with IMPT in many cases. However, PSAS requires patient-specific manufacture, mounting during treatment and storage of the aperture after treatment, so it was not the best way from the view point of patient throughput and a burden on therapists, too. In addition, some fields could not use PSAS due to mechanical collision and limitation of penetration depth. To overcome these

limitations, it is assumed that a movable nozzle and MLC system would improve the lateral penumbra and treatment throughput. Some additional methods have been investigated, for example, to use dynamic collimation with MLC (layer-by-layer collimation)²⁴ or dynamic collimation (spot-by-spot collimation).^{16,25} These methods will come into practical and might improve the dose distribution more. But at present, PSAS system showed dosimetric advantage for shallow region treatment, and in some case, it enables to fulfill dose constraints.

5 | CONCLUSION

We herein reported improvement of dose distribution by using patient-specific apertures with IMPT for shallow depth tumor. The PSAS has some dosimetric advantages for clinical use and is easy to use because it does not require complex machine or control mechanism. Using the PSAS has some demerits from the viewpoint of patient throughput and usability; however, it is useful for clinical application.

ACKNOWLEDGMENTS

We thank the members of NPTC and Hitachi Ltd. who cooperated with this study.

CONFLICT OF INTEREST

The authors have no conflicts of interest directly relevant to the content of this article.

REFERENCES

- ICRU. Prescribing, recording, and reporting proton-beam therapy. ICRU Report No. 78. Bethesda, MD, 2007.
- Kanai T, Kawachi K, Kumamoto Y, et al. Spot scanning system for proton radiotherapy. *Med Phys*. 1980;7:365–369.
- Hashimoto S, Shibamoto Y, Iwata H, et al. Whole-pelvic radiotherapy with spot-scanning proton beams for uterine cervical cancer: a planning study. *J Radiat Res*. 2016;57:524–532.
- Tran A, Zhang J, Woods K, et al. Treatment planning comparison of IMPT, VMAT and 4π radiotherapy for prostate cases. *Radiat Oncol*. 2017;12:10.
- Iwata H, Ogino H, Hashimoto S, et al. Spot scanning and passive scattering proton therapy: relative biological effectiveness and oxygen enhancement ratio in cultured cells. *Int J Radiat Oncol Biol Phys*. 2016;95:95–102.
- Lomax AJ. Intensity modulation methods for proton radiotherapy. *Phys Med Biol*. 1999;44:185–205.
- Lomax AJ, Boehringer T, Coray A, et al. Intensity modulated proton therapy: a clinical example. *Med Phys*. 2001;28:317–324.
- Toshito T, Omachi C, Kibe Y, et al. A proton therapy system in Nagoya proton therapy center. *Australas Phys Eng Sci Med*. 2016;39:645–654.
- Yasui K, Toshito T, Omachi C, et al. A patient-specific aperture system with an energy absorber for spot scanning proton beams: verification for clinical application. *Med Phys*. 2015;42:6999–7010.
- Moteabbed M, Yock TI, Depauw N, Madden TM, Kooy HM, Paganetti H. Impact of spot size and beam-shaping devices on the treatment plan quality for pencil beam scanning proton therapy. *Int J Radiat Oncol Biol Phys*. 2016;95:190–198.
- van de Water T, Lomax AJ, Bijl HP, Schilstra C, Hug EB, Langendijk JA. Using a reduced spot size for intensity-modulated proton therapy potentially improves salivary gland-sparing in oropharyngeal cancer. *Int J Radiat Oncol Biol Phys*. 2012;82:313–319.
- Meier G, Leiser D, Besson R, et al. Contour scanning for penumbra improvement in pencil beam scanned proton therapy. *Phys Med Biol*. 2017;62:2397–2416.
- Kralik JC, Xi L, Solberg TD, Simone CB, Lin L. Comparing proton treatment plans of pediatric brain tumors in two pencil beam scanning nozzles with different spot sizes. *J Appl Clin Med Phys*. 2015;16:5389.
- Charlwood FC, Aitkenhead AH, Mackay RI. A Monte Carlo study on the collimation of pencil beam scanning proton therapy beams. *Med Phys*. 2016;43:1462–1472.
- Hyer DE, Hill PM, Wang D, Smith BR, Flynn RT. A dynamic collimation system for penumbra reduction in spot-scanning proton therapy: proof of concept. *Med Phys*. 2014;41:1701.
- Moignier A, Gelover E, Wang D, et al. Theoretical benefits of dynamic collimation in pencil beam scanning proton therapy for brain tumors: dosimetric and radiobiological metrics. *Int J Radiat Oncol Biol Phys*. 2016;95:171–180.
- Dowdell SJ, Clasie B, Depauw N, et al. Monte Carlo study of the potential reduction in out-of-field dose using a patient-specific aperture in pencil beam scanning proton therapy. *Phys Med Biol*. 2012;57:2829–2842.
- Jelen U, Bubula ME, Ammazalorso F, Engenhardt-Cabillic R, Weber U, Wittig A. Dosimetric impact of reduced nozzle-to-isocenter distance in intensity-modulated proton therapy of intracranial tumors in combined proton-carbon fixed-nozzle treatment facilities. *Radiat Oncol*. 2013;8:218.
- Both S, Shen J, Kirk M, et al. Development and clinical implementation of a universal bolus to maintain spot size during delivery of base of skull pencil beam scanning proton therapy. *Int J Radiat Oncol Biol Phys*. 2014;90:79–84.
- Hirayama S, Takayanagi T, Fujii Y, et al. Evaluation of the influence of double and triple Gaussian proton kernel models on accuracy of dose calculations for spot scanning technique. *Med Phys*. 2016;43:1437.
- Schaffner B, Pedroni E, Lomax A. Dose calculation models for proton treatment planning using a dynamic beam delivery system: An attempt to include density heterogeneity effects in the analytical dose calculation. *Phys Med Biol*. 1999;44:27–41.
- Pflugfelder D, Wilkens JJ, Oelfke U. Worst case optimization: a method to account for uncertainties in the optimization of intensity modulated proton therapy. *Phys Med Biol*. 2008;53:1689–1700.
- Park PC, Zhu XR, Lee AK, et al. A beam-specific planning target volume (PTV) design for proton therapy to account for setup and range uncertainties. *Int J Radiat Oncol Biol Phys*. 2012;82:1–8.
- Kanematsu N, Endo M, Futami Y, et al. Treatment planning for the layer-stacking irradiation system for three-dimensional conformal heavy-ion radiotherapy. *Med Phys*. 2002;29:2823–2829.
- Moignier A, Gelover E, Smith BR, et al. Toward improved target conformity for two spot scanning proton therapy delivery systems using dynamic collimation. *Med Phys*. 2016;43:1421–1427.